Stony Brook University

OFFICIAL COPY

The official electronic file of this thesis or dissertation is maintained by the University Libraries on behalf of The Graduate School at Stony Brook University.

© All Rights Reserved by Author.

Structural characterization of individual domains of an energy dependent mitochondrial protease

A Thesis Presented

by

Faiza Sheikh

to

The Graduate School

in Partial Fulfillment of the

Requirements

for the Degree of

Master of Science

in

Biochemistry and Cell Biology

Stony Brook University

December 2013

Stony Brook University

The Graduate School

Faiza Sheikh

We, the thesis committee for the above candidate for the

Master of Science degree, hereby recommend

acceptance of this thesis.

Dr. Steven E. Glynn – Thesis Advisor
Assistant Professor, Department of Biochemistry and Cell Biology

Dr. A. Wali Karzai Ph.D. – Second Reader
Associate Professor, Department of Biochemistry and Cell Biology

This thesis is accepted by the Graduate School

Charles Taber
Dean of the Graduate School

Abstract of the Thesis

Structural characterization of individual domains of an energy dependent mitochondrial protease

by

Faiza Sheikh

Master of Science

in

Biochemistry and Cell Biology

Stony Brook University

2013

The ATP- dependent i-AAA protease pulls in and unwinds improperly folded and short-lived membrane proteins in order to maintain the integrity of the mitochondrial inner membrane. The i-AAA protease consists of an N-terminal domain, a single trans-membrane domain, a AAA ATPase domain and a metalloprotease domain. The role of the AAA domain is to unfold and translocate targeted proteins to protease domain where they are degraded. To further our understanding of the mechanism of this important enzyme, I sought to isolate and gain structural information on the individual domains of the i-AAA protease from the thermophilic eukaryote *Myceliophthoya thermophile*. I used sequence alignments to determine domain boundaries for the protease domain based on the structure of a related enzyme, FtsH. A construct containing this domain was cloned and expressed but did not express well enough on the large scale to move forward with crystallization. A construct containing the isolated N-terminal domain was expressed and purified in large quantities and used in crystallization trials. The high solubility of the protein prevented crystallization so I used reductive methylation to modify surface lysine

residues and reduce solubility. Crystallization trials with this modified protein have yielded promising hits. Circular dichroism measurements indicated that the protein is largely alpha-helical in structure and chemical denaturation with urea suggested that the protein is stable with a mid-point of unfolding between 4 and 5 M urea.

This thesis is dedicated to Shaikh I Haq, Iffat Inam and Steven Glynn

Table of Contents

List of Figures

List of Tables

List of Abbreviations

AAA	ATPases Associated with diverse cellular Activities
i-AAA	Intermembrane- ATPases Associated with diverse cellular Activities
m-AAA	Matrix- ATPases Associated with diverse cellular Activities
IPTG	isopropylthio-β-galactoside
BME	2-mercaptoethanol
MES	2-(*N*-morpholino)ethanesulfonic acid
CD	circular dichroism
PMSF	phenylmethylsulfonyl fluoride
Cox2p	cytochrome c oxidase
MW	molecular weight
S	soluble fraction
IS	insoluble fraction
Pre	Pre-induction
Post	Post-induction
FT	flow through
W	wash
mtDNA	mitochondrial DNA
ABC	dimethylamine-borane complex

Acknowledgements

I would like to thank my thesis advisor Dr. Steven E. Glynn, without his help it would not be possible to finish things on time. His guidance, suggestions and patience encouraged me through out my research. Moreover, I am thankful to all my lab members Hui, Caitlin, Anthony and Boijan for supporting me and polishing my lab skills. I would also like to thank Dr. Karzi for taking his time out for my thesis and for serving as my second reader. Moreover, I would like to thank my parents for all the sacrifices they have done for me so far, my brother and sister for cheering me and Furqan for supporting me and loving me so much. Last but not the least all my friends for pushing me and advising me through out my life.

1. Introduction

1.1. Mitochondria

Mitochondria are the energy generator for the cell. They are thought to have originated from an ancient symbiosis that resulted when a nucleated cell engulfed an aerobic prokaryote (1). They are designed to break down nutrients, and release the energy for the cell to carry out various cellular activities. They divide independently of the cell in which they reside (1). To successfully meet these energy requirements, thousands of mitochondria exist in a single cell. The quantity of mitochondria found in a cell depends on its specific function. These organelles replicate by dividing in two, using a process similar to the simple, asexual form of cell division employed by bacteria (1). Mitochondria do synthesize a few of their own proteins, but the majority of the proteins they require are encoded in the nuclear genome. These include the enzymes, the proteins involved in DNA replication and transcription, and ribosomal proteins (1). Mitochondria contain compartments defined by membranes: an inner membrane containing the matrix covered by an outer membrane, with a small intermembrane space in between (Figure 1.1). The outer membrane has many protein-based pores that are big enough to allow the passage of ions and molecules. In contrast, the inner membrane has much more restricted permeability and involved in electron transport and ATP synthesis (1). Thousands of precursor proteins are imported in these mitochondrial compartments.

Despite the diminutive size of the mitochondria genome, mitochondria DNA (mtDNA) mutations are an important cause of inherited disease. The increasing ease with which the mitochondrial genome can be analyzed has helped to recognize mtDNA disorders as a common cause of genetic disease (2). In addition, there is increasing evidence from animal models (3) and

human studies (4) that acquired mtDNA mutations and mitochondrial dysfunction are involved in ageing and diabetes (5,6). Mitochondrial disease can also arise from nuclear gene disorders because most protein involved in mitochondrial metabolism and all those involved in mtDNA maintenance are nuclear-encoded (7,8,9).

1.2. Mitochondrial inner membrane

Most of a cell's ATP is produced in the inner membrane of mitochondria. Without this energy the multicellular eukaryotes would have to depend on the energy generated from glycolysis (10). The inner membrane is the anchor for electron transport and oxidative phosphorylation proteins and also contains transport proteins for passing common metabolites, such as ATP, ADP, pyruvate, Ca^{2+}, and phosphate (11). The inner membrane of mitochondria is much richer in proteins, up to 70% protein by mass, than the outer-membrane and allows only O_2, CO_2, and H_2O to freely pass (11). In addition, the matrix of the inner mitochondrial compartment contains high concentrations of oxidative metabolic enzymes as well as the mitochondrial DNA, RNA, and ribosomes for making mitochondrial proteins (11). The integrity of the inner membrane is important for the function of the mitochondrion, which harness energy from the chemical gradient it creates across the membrane, therefore, strict quality control becomes the necessity.

1.3. ATP-dependent proteases of mitochondria

ATP-dependent proteases mediate the complete degradation of dispensable mitochondrial proteins. Several ATP-dependent proteases have been identified in different sub compartments of mitochondria (Figure 1.2). Studies in the yeast *Saccharomyces cerevisiae* revealed a double

function of ATP-dependent proteases in mitochondria (12). Firstly, they constitute a quality control system and prevent the possibly deleterious accumulation of non-assembled and misfolded polypeptides in the organelle (12). Secondly, the selective proteolysis of some mitochondrial proteins by ATP-dependent proteases appears to be crucial for mitochondrial biogenesis (12).

1.4. AAA proteases in the mitochondrial inner membrane

Proteolysis is mediated by membrane-embedded ATP-dependent AAA proteases form ring-like assemblies (figure 1.3), which comprise a conserved protein family with homologues in various organisms, including bacteria, plants, yeasts and humans (13,14,15). Two AAA proteases have been identified in the mitochondrial inner membrane of *S. cerevisiae* (16,17,18,19). Both proteases are composed of homologues subunits and form high-molecular-mass complexes of approximately 1 MDa (20,21). The catalytic sites, however, are exposed to opposite membrane surfaces, the matrix and the intermembrane space sides, and are accordingly termed m- and i-AAA protease (figure 1.4).

AAA proteases are highly conserved energy-dependent proteolytic machines; they conduct the quality check of respiratory chain and ATP synthase complexes (22,23). An ATPase domain has chaperone-like properties, which assists in the interaction with un-folded membrane proteins so as to successfully ensure the specificity of the proteolysis (24,25). A proteolytic domain, which is present at the C-terminus, has metallopeptidase activity. A degradation of inner membrane polypeptides requires ATP hydrolysis. Conformational changes in i-AAA are induced through the process of ATP binding and hydrolysis (22,26). These changes control the accessibility of the proteolytic sites and meditate unfolding of substrate polypeptides, which

allows consequent degradation by the proteolytic domain (27). Additionally, conserved loop regions within the central channel formed by the ATPase subunits have been demonstrated to be involved in substrate binding (28). The expression of mitochondrially-encoded subunits of respiratory chain complexes and their assembly are strictly reliant on ATP-dependent proteolysis. Therefore, these proteases exhibit multiple functions to maintain cellular respiratory competence in a strict manner (figure 1.5).

1.5. The m-AAA protease

The m-AAA protease consists of multiple copies of the ATP-dependent metallopeptideases Ytal0p (Afg3p) (20,29) and Yta12p (Rcalp) (18,30). A small N-terminal and a large C-terminal domain containing the catalytic sites are exposed to the matrix (23). The m-AAA protease is essential for the maintenance of oxidative phosphorylation (18,20,29,31). The expression of the mitochondrially encoded respiratory chain subunits Cox1p and Cob is under the proteolytic control of the m-AAA protease (31). It is also believed that m-AAA protease might be involved in the proteolytic activation of RNA maturases (32). The activity of m-AAA is required to ensure the expression of two mitochondrial mosaic genes coding for essential respiratory chain subunits (33). In addition, the m-AAA protease also affects the post-translational assembly of respiratory chain complexes and F_1F_0-ATP synthase (31,34). Two orthologues of yeast m-AAA protease subunits have been identified in humans (35,36).

1.6. The i-AAA protease

The i-AAA exerts ATP- dependent metalopeptidase activity (21). It consists of Yme1p (Yta11p) that is highly homologous to Yra10p and Yta12p. Yme1p contains one transmembrane

segment. N-terminal domain consisting of 170 amino acid residues is present in the matrix space and a C-terminus domain with the catalytic sites is facing the intermembrane space (13). Mitochondrial i-AAA protease Yme 1 mediates Atg32 processing and acts as an important regulatory mechanism of cellular mitophagy activity (20). Moreover, the only reported substrate of i-AAA protease is non-assembled subunit 2 of cytochrome c oxidase (Cox2p) (38,39,40), illustrating the quality control function of the protease in the inner membrane.

1.7. Domain structures of AAA-protease subunits

Both m-AAA and i-AAA proteases form a large complexes built up of homologous subunits in all eukaryotic cells with the sequence identities of >40% between the bacterial, yeast, plant and human members (41). The m-AAA protease is a hetero-oligomeric complex of Yta10 (Afg3) and Yta12 (Rcal) subunits in yeast (23) and AFGL2- and paraplegin-subunits in humans (42), whereas Yme1 subunits most likely form homooligomeric i-AAA protease in mitochondria of both organisms (13). All known subunits of AAA protease share a common domain structure. First comes the N-terminal region, which is regarded as the accessory domain of AAA proteases, critical for substrate recognition (43). The substrate proteins come in contact with the N-domains during binding and translocation steps, and such contact may produce allosteric stabilization of the association of AAA domain with protease domain (43). This region is followed by one or two transmembrane segements, which anchor the protein to membranes. Then comes the AAA domain, which is followed by the proteolytic domain that is considered the most conserved parts of AAA proteases (figure 1.6). The proteolytic domain of AAA proteases harbors a consensus metal binding site, which forms the proteolytic center identifying AAA proteases as metallopeptidases.

1.8 Consequences of inactivation of AAA proteases

Inactivation of AAA proteases causes severe defects in various organisms (figure 1.5) including neurodegeneration in humans, most likely reflecting regulatory functions of these proteases crucial for the biogenesis and homeostasis of mitochondria (33). Moreover, point mutations in the proteolytic center of i-AAA (Yme1p) or deletion of the entire *YME1* gene result in identical pleiotropic defects in *S*. *cerevisiae* (38,44,45). Cells lose their respiratory competence at elevated temperature and accumulate mitochondria with punctate, non-reticulated morphology (33). In addition, mutations in m-AAA cause an autosomal recessive form of hereditary spastic paraplegia (35). Deficiencies in mitochondrial oxidative phosphorylation were also observed in these cells (33). Examination of the molecular mechanisms of membrane-protein turnover in the cell can be attained through the structural analysis of both the i-AAA and m-AAA. My investigations are focused on the purification, characterization and crystallization of the protease domain and N-terminal domain of i-AAA protease. The detailed structure analysis of these two domains will revel the important part played in the recognition and the degradation of the misassembled membrane proteins.

Figures

Figure 1.1

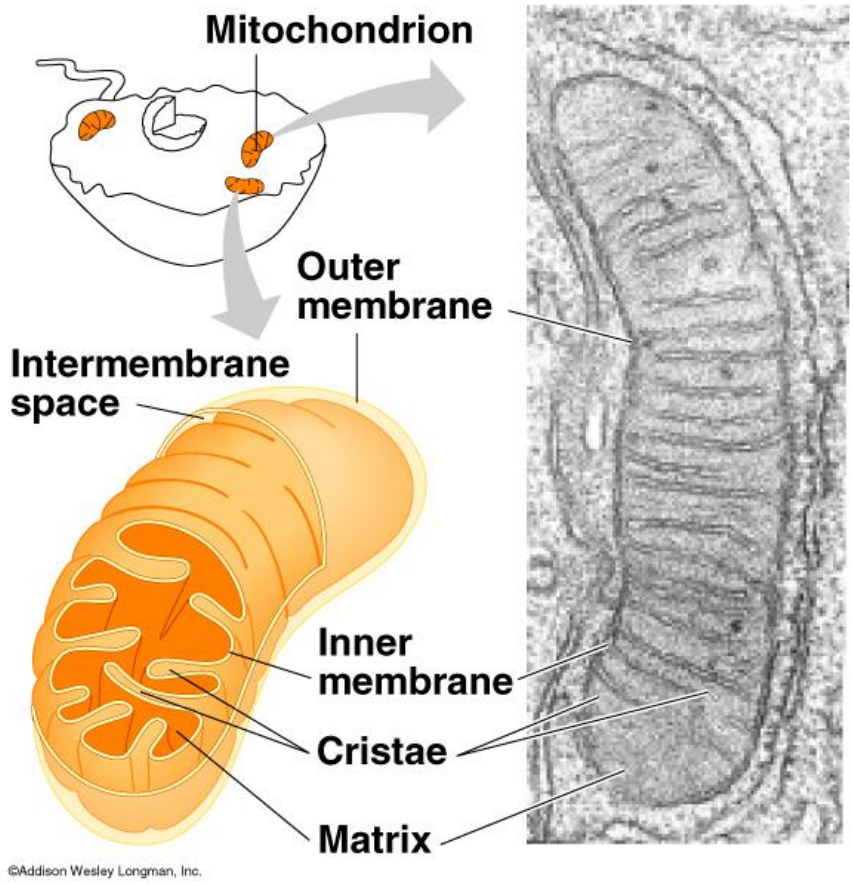

Figure 1.1*: *Schematic representation of Mitochondria. The figure on top left corner is showing the presence of mitochondria in the cytoplasm of a cell. The figure on the lower right showing the mitochondrial structural features such as outer membrane, inner membrane, intermembrane space, cristae and matrix. The figure of right is an electron microscopic image of mitochondrial structure features.
[Figure adapted from http://bioserv.fiu.edu/~walterm/fallspring/cell_components/cell_talk.html]

Figure 1.2

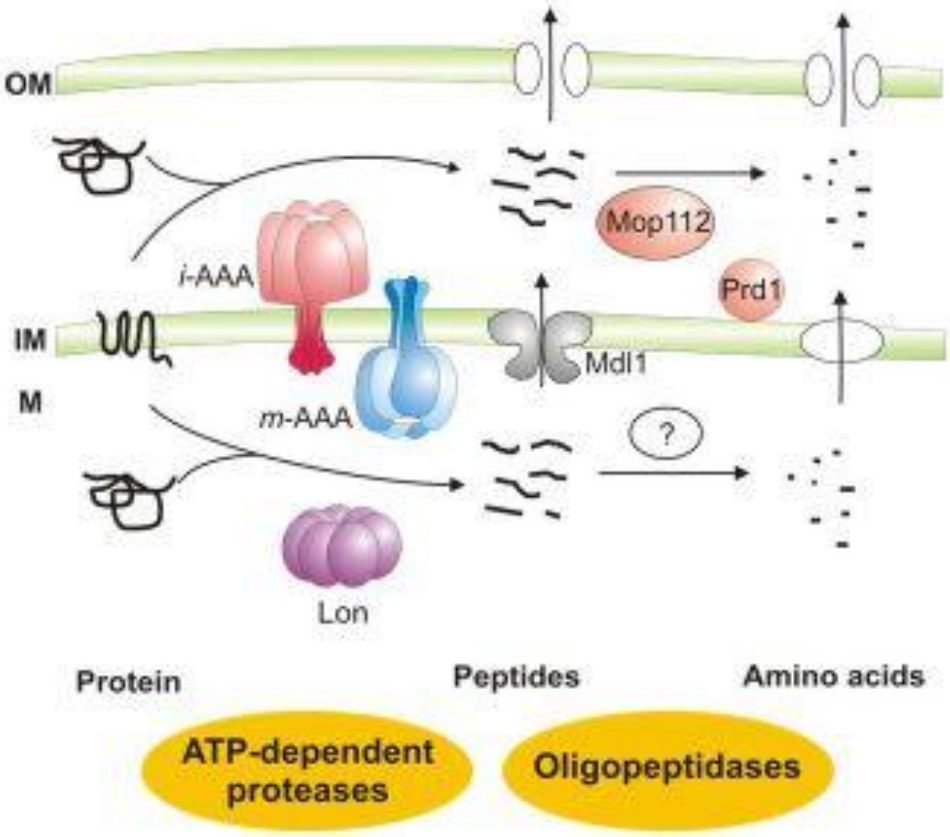

Figure 1.2**:** *Proteolytic pathways in mitochondria of S. cerevisiae*. Highly conserved energy-dependent proteolytic machines, such as i-AAA, m-AAA and Lon, in the inner membrane of mitochondria, conduct the quality check with in the mitochondria. [Figure adapted from http://www.genetik.uni-koeln.de/groups/Langer/proteolysis.html]

Figure 1.3

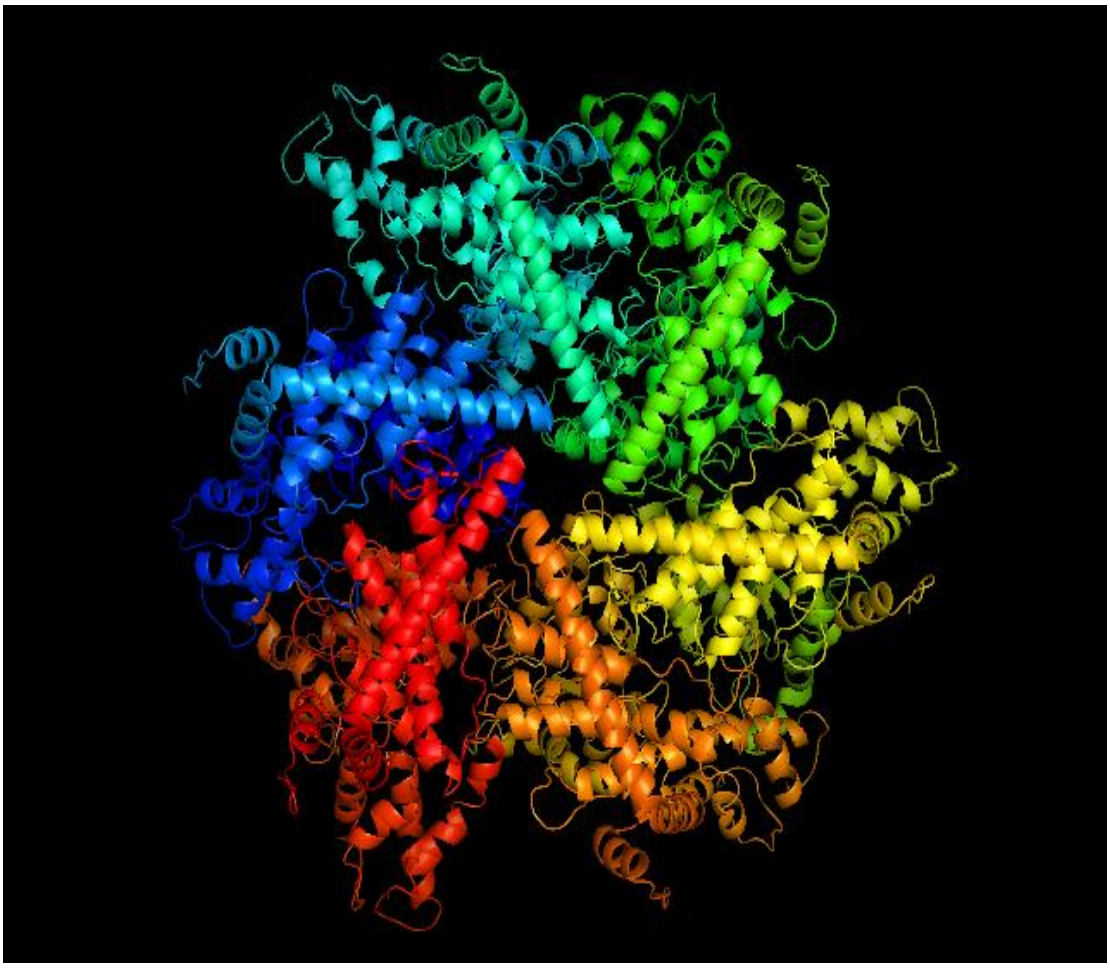

Figure 1.3*: *Model of the hexameric ring of AAA-domains of the i-AAA protease Yme1
[Figure adapted from
http://www.genetik.uni-koeln.de/groups/Langer/proteolysis.html]

Figure 1.4

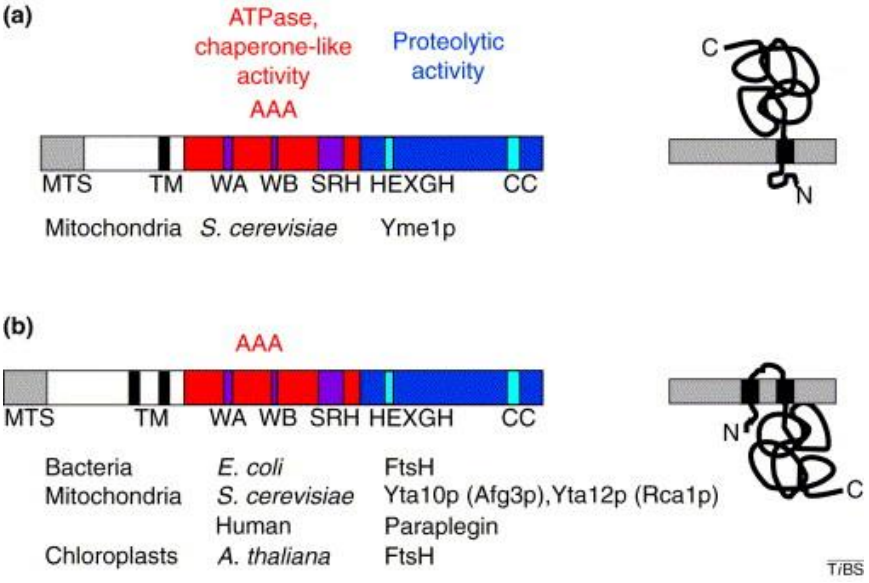

Figure 1.4*: *Domain structures of AAA-protease subunits. Two subunit classes can be distinguished, which contain one (a) (Class I) or (b) two (Class II) transmembrane segments (TMs) and consequently differ in their membrane topology. The degree of sequence conservation is similar within each class and between the classes. Representative examples for both classes are given. Abbreviations used: AAA, ATPase domain; CC, coiled-coil region; HEXGH, metal-binding site; MTS, mitochondrial targeting signal; SRH, second region of homology
[Figure adapted from Thomas Langer. 2000]

Figure 1.5

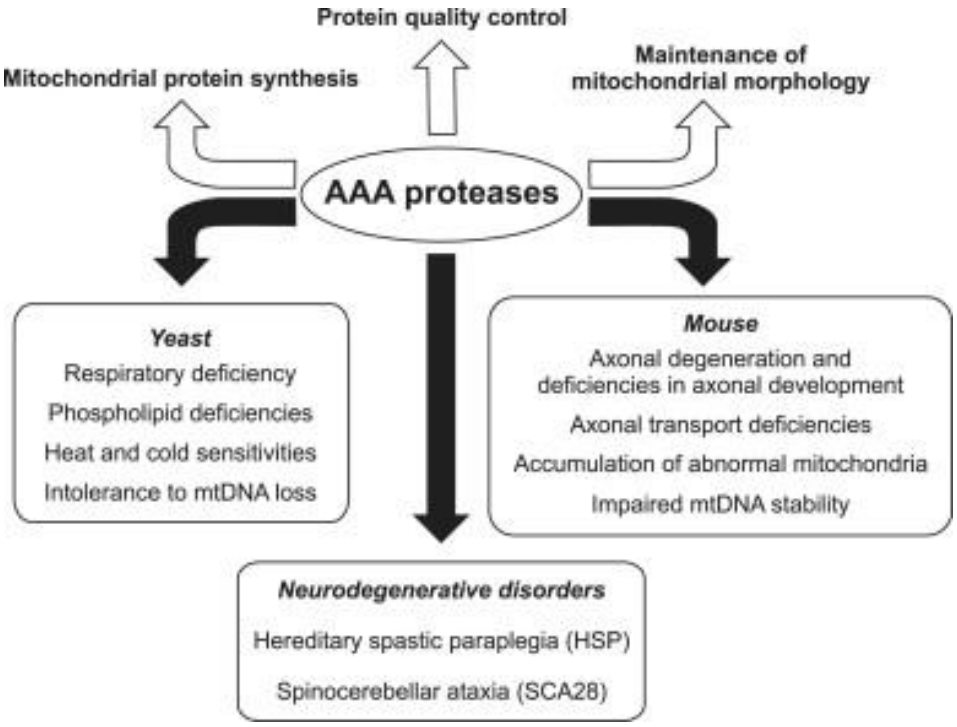

Figure 1.5*: *Roles of AAA proteases in mitochondria. Upper panel: versatile activities of AAA proteases. Lower panel: consequences of the impaired activity of AAA proteases in yeast, humans and mice.
[Figure adapted from Takashi Tatsuta et al. 2009]

Figure 1.6

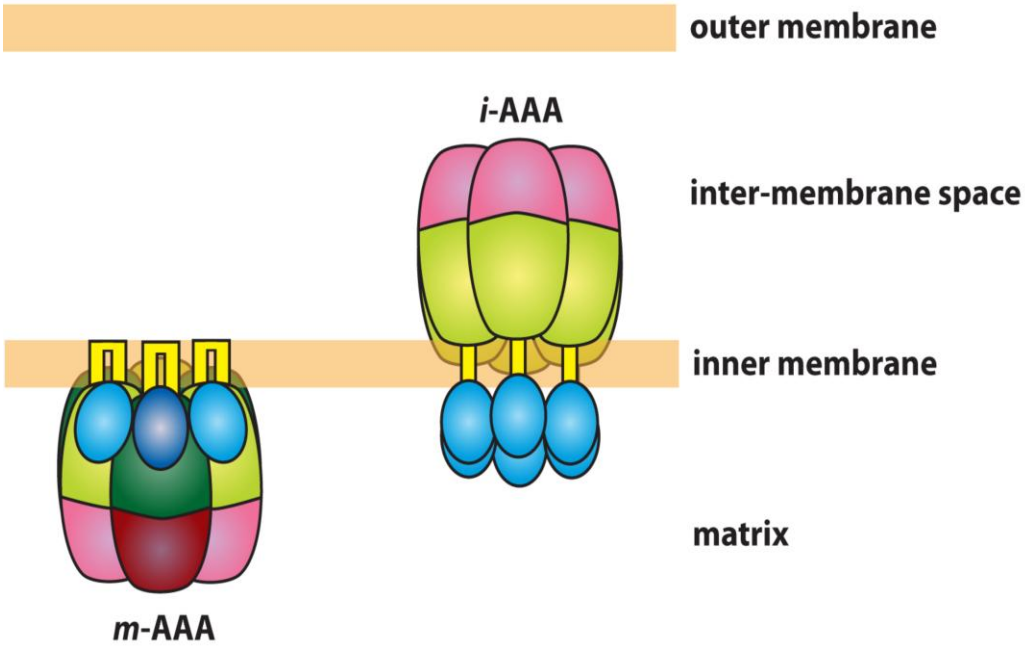

Figure 1.6*: *Schematic representation of different domains of AAA proteases. The m-AAA and i-AAA have their catalytic domains in matrix and intermembranal space respectively. The blue region represents the N-terminal domain, followed by transmembrane segments in yellow. The AAA domain is colored in green, followed by protease domain in pink.

2. Materials and Methods

2.1. Cloning, Amplification and Transformation

cDNA was obtained from *Myceliophthora thermophile*, forward and reverse primers were designed to generate a protease domain fragment of i-AAA. The forward primer sequence is 5'-TACTTCCAATCCAATGCAATCACGCCCAAGGAGAAGG - 3' and the reverse primer sequence is 5'-TTATCCACTTCCAATGTTATTATCATTCATCCCTTTCCCCATTTCC – 3'. Underlined tags were added to both the forward and reverse primers to make them suitable for ligation-independent cloning (LIC). The PCR reaction was performed including 35 µl Nuclease-Free water, 10 µl 5x Phusion Buffer, 1 µl of 10 mM dNTPs, 0.25 µl of 10 Forward Primer, 0.25 µl of 10 of Reverse Primer, 1.5 µl Template DNA, 1.5 µl DMSO, and 0.5 µl DNA Polymerase. PCR was performed using the following conditions: initial denaturation for 30 seconds at 98°C, denaturation for 20 seconds at 98°C, annealing for 20 seconds at 63.5°C, elongation for 45 seconds at 72°C. The cycle from denaturation to elongation was repeated 30 times with a final elongation step of 10 minutes at 72°C. To confirm the successful amplification the PCR products were run on a 0.8 % agarose gel with ethidium bromide. The band corresponding to the protease domain was excised from the gel and purified using the Qiagen QIAquick Gel Extraction kit. The concentration of the sample was checked by UV absorbance at 280 nm using the NanoDrop spectrophotometer.

The LIC method was used to ligate the cDNA fragment into designed LIC vectors. The LIC vectors bearing an N-terminal polyhistidine tag (2BT), an N-terminal Sumo tag (2ST), or an N-terminal MBP tag (2MT) were linearized with the restriction enzyme Ssp1. The linearization was conducted in three tubes containing 5 µl of NE Buffer 4, 2 µl of Ssp1, 43 µl of 2BT in one

tube, 43 µl 2ST in the second tube, and 35 µl of 2MT with 8 µl of water in the third tube. The tubes were placed in a 37°C incubator for 3 hours. To confirm linearization the samples were run on a 0.8 % agarose gel. The bands corresponding to the three vectors were excised from the gel and purified using the Qiagen QIAquick Gel Extraction kit. The concentration of the samples was checked by UV absorbance at 280 nm using the NanoDrop spectrophotometer. After linearization large single-strand overhangs were generated on both the vectors and inserts by treatment with T4 DNA polymerase in the presence of limiting concentration of dNTPs. For vectors, 10 µl of linearized vector, 2µl of T4 buffer, 2µl of dGTP (25 mM), 1 µl of DTT (100 mM), 0.2 µl of T4 Polymerase enzyme and 4.8 µl of water were added together. For the insert 5 µl of purified PCR, 2 µl of T4 buffer, 2 µl of dCTP (25 mM), 1 µl of DTT (100 mM), 0.2 µl of T4 Polymerase enzyme and 9.8 µl of water were added together. Both the insert and the vector were then incubated at 22°C for 40 minutes, and then heat-denatured at 75°C for 20 minutes. Next 5 µl of T4 treated vector was combined with 5 µl of T4 treated insert in total volume of 20 µl. The mixture was incubated for 30 minutes at room temperature to anneal.

The 10 µl of the mixture was transformed into the DH5α cloning strain of E. coli. 1ml LB was added and the mixture was shake at 37°C for 1 hour. The cells were spun down for 1 minute at 13k rpm, and 800 µl of supernatant was discarded. The cells were re-suspended in the remaining media, and then 150 µl of the transformed cells were spread on the agar plates with ampicillin (100 mg/ml) and incubated overnight at 37°C. The following day, colonies were selected and grown overnight in 5 ml LB medium with ampicillin (100mg/ml) in a shaker at 37°C. Plasmid was extracted using a Qiagen QIAprep Spin Miniprep Kit. Correct sequences were verified by DNA sequencing. Moved on with 2MT and transformed the cells in BL21* the

expression strain of E.coli. Spread 150 µl of the sample on an agar plate with ampicillin (100mg/ml) and placed it in 37°C incubator for overnight.

2.2. Expression

2.2.1. Small-Scale Expression

Colonies containing the transformed plasmid were inoculated into 5ml LB culture tube with ampicillin (100mg/ml) and incubated with shaking at 37°C shaker for 4 hours. 1ml of culture was removed as a pre-induction control. The cells were centrifuged and the pellet was resuspended in 90 µl lysis buffer containing 8M Urea, 20 mM Tris (pH 8.0), 400 mM NaCl, 100 mM KCl, and 10% glycerol, then added 30 µl 4X SDS loading buffer and incubated at 95°C for 10 minutes. IPTG was added to induce expression at a final concentration of 1mM and the protein was expressed at 37°C for 3 hours. 1 ml of culture was removed after 3 hours and treated in the same way as the pre-incubation sample. To confirm the successful expression of the cells the pre and post induction samples were resolved by 12% SDS-PAGE.

2.2.2. Large Scale-Expression

50 ml of LB was inoculated in the presence of ampicillin (100mg/ml) and grown at 37°C overnight. 5ml of overnight culture was inoculated into 1L LB containing ampicillin (100mg/ml). The culture was grown at 37°C until the ODC at 600 nm reached 0.6. IPTG was added to a final concentration of 1mM to induce expression and the culture was moved to 30°C for 3 hours. After 3 hours the culture was centrifuged at 4K rpm for 30 minutes to pellet the cells. The pellet was re-suspended in 25 ml of 0.1 M NaCl to wash the cells and centrifuges for

20 minutes at 3K rpm using a bench top centrifuge. The supernatant was discarded and the pellet was frozen at -80°C.

2.3. Protein Purification

Pelleted cells were resuspended in 25 ml buffer A containing 1 mM PMSF. The resuspended cells were lysed using a french press homogenizer. After lysing 1 µl of Benzonase was added to degrade nucleic acids. The lysed cells were centrifuged at 15000 rpm for 30 minutes to pellet cell debris. The supernatant was added to 4 ml of HisPur nickel slurry and incubated for 45 minutes with agitation. The resin was placed in a gravity column and the flow through was collected. The resin was washed two times with buffer A. Bound protein was eluted 5 ml of buffer B (pH 7.5) containing 20 mM HEPES, 400 mM NaCl, 100 mM KCl, 500 mM imidazole, 10 mM 2-mercaptoethanol and 5 % glycerol and collected in 0.5ml fractions. Fractions containing protein were identified by assay with Bradford reagent. Fractions containing the highest concentration of protein were pooled and concentrated using a spin concentrator with a 3 kDa cutoff. Up to 2 mls of sample was loaded onto a Superdex 200 26/60 gel filtration column equilibrated with buffer C containing 10 mM Tris (pH 8), 100 mM NaCl, and 1 mM DTT. 2 ml fractions were collected and checked for purity by SDS-PAGE. The fractions containing target protein were pooled and concentrated and the final protein concentration was measure by absorbance at 280 nm

For N-terminal domain purification followed the similar steps except the buffers compositions were different. For the resuspension of the pellet and for the washes used buffer D containing 20 mM HEPES (pH7.5), 100 KCl, 400 NaCl, 5 % glycerol, 10 mM Imidazole and 10 mM 2-mercaptoethanol. For the elution of the protein from the Nickel column used buffer E

containing 20 mM HEPES (pH 7.5), 100 mM KCl, 400 mM NaCl, 5% glycerol, 500 mM Imidazole and 10 mM 2-mercaptoethanol. Gel filtration was equilibrated with buffer F containing 10 mM Tris (pH 8.0), 100 mM NaCl and 1 mM DTT.

2.4. Crystallization Trails

Crystallization trials were performed using the NT8 drop setter (Formulatrix) by mixing 0.1 µl of the protein solution (83mg/ml) with an equal volume of precipitant and equilibrating against the same precipitant at 290K. The proteins were screened with pre-mixed crystallization screens including Qiagen Nextal JCSG + suite, Qiagen Nextal Protein Complex Suite, Hampton SaltRx, Hampton PEFRx, and Hampton Index. The crystallization trays were incubated at 20°C.

2.5. Lysine methylation

The method used is derived from that published previously (47). The lysine methylation reaction is performed overnight in 50 mM HEPES (pH7.5), 250 mM NaCl at protein concentration of 1mg/ml. Twenty microliters freshly prepared 1 M dimethylamine-borane complex (ABC) and 40 µl 1M formaldehyde (made from 37% stock) are added per ml of protein solution, and the reaction is gently mixed and incubated at 4°C for 2 hr. An additional 20 µl ABC and 40 µl of formaldehyde are added and the incubation continued for 2 hr. Then a final aliquot of 10 µl of ABC is added and the reaction is incubated overnight at 4°C. The next day, in order to remove any precipitation formed, the sample is spun down for 10 minutes at 14 K rp, and then centrifuged before purification of the soluble methylated proteins by size-exclusion chromatography (Superdex 200 on FPLC system). The column is pre-equilibrated in 20 mM Tris-HCl (pH7.5), 200 mM NaCl. Appropriate peak fractions are pooled and concentrated in

centrifugal concentrators (Vivascience) to appropriate concentrations. Crystallization experiments were set up immediately.

2.6. Circular Dichroism (CD)

Circular dichroism spectra were measured using a Olis RSM 1000 UV/Vis [NIR] rapid-scanning spectrophotometer. A rectangular cuvette with path length 1mm, exterior width 12.5 mm, and length 3.5 mm, interior width 10 mm, and length 1 mm and the height 45 mm was chosen. The stocks solutions including 8 M and 12 M Urea, and 0.5 mM sodium phosphate buffer of pH 8 were prepared. Buffers were prepared with increasing concentration of urea. Table 1 displays the quantity of stock solutions utilized to prepare the buffers. The starting concentration of the protein sample was 3.86 mg/ml diluted to 0.2mg/ml with eight different concentration buffers; table 2 displays the preparation of the samples. The samples were collected from a wavelength of 200 nm to 260 nm. The scale for Y-axis was selected from -30 to 30 (ellipticity per residue $\times 10^3$). A baseline was collected before running every sample, and 60 points were collected in total. Moreover, an average of 3 scan was performed and analyzed.

Table 1: The quantity of stock solutions used to prepared eight buffers containing increasing urea concentration.

Concentration Of Urea (M)	**0.5 M Sodium Phosphate (Ml)**	**8 M Urea (ml)**	**12 M Urea (ml)**	**H_2O (ml)**
1	1	6.25	-	42.75
2	1	12.50	-	36.50

3	1	18.75	-	30.25
4	1	25.00	-	24.00
5	1	31.25	-	17.75
6	1	37.50	-	11.50
8	1	-	33.33	15.67

Table 2: The samples were prepared for circular dichroism spectroscopy by combining 284 µl of the buffer and 16 µl of protein

Concentration of Urea Buffer (M)	**0**	**1**	**2**	**3**	**4**	**5**	**6**	**7**	**8**
Buffer (µl)	284	284	284	284	284	284	284	284	284
Protein sample (µl)	16	16	16	16	16	16	16	16	16
Total Volume (µl)	300	300	300	300	300	300	300	300	300

3. Results and Discussion

3.1. Cloning and expression of protease domain of i-AAA

The aim of this project was to characterize the protease domain of i-AAA with three main purposes. The first purpose was to analyze the primary sequence in order to determine the domain boundaries. The second purpose was to clone the protease domain by PCR into an expression vector. The third purpose was to express and purify the protein and finally, to step up crystallization trials and perform biochemical assays on the purified proteolytic domain.

3.1.1. Evaluation of primary sequence and selection of domain boundaries

In order to determine domain boundaries, firstly, the primary sequences of related proteases were aligned using BLAST (48) and CLUSTALW (49). These alignments indicated that the most closely related protease whose structure has been determined is the bacterial enzyme FtsH (figure 3.1). Consequently, we performed a structural alignment of FtsH with the amino acid sequence of the i-AAA protease (figure 3.2).

Based on the structure of FtsH, we determine that the proteolytic domain of the enzyme span residues 412-600, which correspond to residues 490-746 in the sequence-alignment with the i-AAA protease. Importantly these domain boundaries contain the conserved HEXXH motif that coordinates the catalytic zinc ion and is responsible for the cleavage of peptide bonds. This designed construct contains 257 amino acids with the molecular weight of 32 kDa.

3.1.2. Construction of ligation-independent cloning vectors for expression and purification of recombination proteins in *Escherichia.coli*

After the selection of domain boundaries, forward and reverse primers were designed in order to amplify the protease domain from the i-AAA of *M*. *thermophile*. PCR was performed to amplify the DNA and the PCR product was resolved on a 0.8 % agarose gel. Inspection of the gel under UV light revealed two significant bands (data not shown). One band ran between the 1 kbp and 0.5 kbp molecular weight markers corresponding to expected size of 771 bps for the correct product. The second band was of much lower molecular weight, likely corresponding to primer dimers. The band corresponding to current molecular weight was cut out and extracted using the Qiagen Gel Extraction Kit.

LIC vectors were linearized by cleavage with the restriction enzyme Ssp1 and linearized products were resolved on the gel (Figure 3.3). A clear band was present for N-terminal MBP tag (2MT) and for an N-terminal Sumo tag (2ST) vectors but for an N-terminal polyhistidine tag (2BT) two bands were observed. Probably, the Ssp1 treatment did not cut the 2BT as precisely as it cut the other two. Fresh 2BT was treated with Ssp1 and this time the restriction enzyme cut the vector precisely. The 2ST, 2MT and 2BT vectors were purified using a Qiagen Gel Extraction Kit. Both vectors and insert were treated with T4 DNA polymerase in the presence of a limiting nucleotide as outlined in materials and methods. This treatment created long complementary single stranded over hanged in the vector and insert. The annealed constructs were transformed by heat shock into *E.coli* DH5α. Plasmids were purified from colonies after selection with ampicillin and sequenced to verify the successful insertion of the protease domain fragment into 2ST, 2MT, and 2BT to create construct $2ST^{490\text{-}746}$, $2MT^{490\text{-}746}$, and $2BT^{490\text{-}746}$.

Small-scale expression was performed with $2BT^{490\text{-}746}$ plasmid after induction with IPTG and was resolved on a 12 % SDS-PAGE gel. The gel confirmed the expression of the protease domain fragment fused to His tag at the N-terminus (figure 3.4). However, large-scale expression

of the construct was unsuccessful (figure 3.4). Since the protein was not expressing at large-scale I moved to study the N-terminal domain of the i-AAA protease.

3.2. Expression and purification of N-terminal domain of i-AAA

Previously, a construct bearing residues 56 to 196 of *Myceliophthora thermophile* i-AAA protease had been cloned and successfully expressed and purified. However, the purified protein was shown to be susceptible to degradation. Mass spectrometry analysis of the degradation products revealed a cleavage side at residue 178 (A. Rampello personal communication). A possible explanation of this observation is that the C-terminal end of the N-terminal domain unstructured and therefore susceptible to proteolysis. To prevent degradation a new construct was produced lacking the c-terminal eighteen amino acid of this domain

The N-terminal domain was cloned in to 2BT vector and the successful insertion of it was confirmed by sequencing ($2BT^{56-178}$). I performed a small-scale expression test on this construct (figure 3.5), followed by expression in 1 L of BL21 (DE3) (figure 3.5). Expressed protein was purified using nickel affinity chromatography and gel filtration (see material and methods) (figure 3.6).

3.2.1. Crystallization of N-terminal domain of i-AAA

Purified protein was concentrated to 25mg/ml and crystallization trials were step up. However, almost all the drops were clear after 2 weeks, which suggest that the concentration of the protein was two low to achieve crystallization. To improve the chances of producing crystals, the protein was repurified from 2 L of culture (figure 3.7). A single peak was seen in a gel filtration spectrum and was compared with the standard spectrum of superdex 200 (figure 3.8).

This time the final concentration was 83 mg/ml. Crystallization trials were set up, and two possible hits were observed. The conditions of the two hits are mentioned in table 3 and table 4.

Table 3: Conditions of a possible hit 1 of crystallization trial

Type	**Name**	**Stock Conc.**	**Conc.**	**Units**	**pH**
Precipitant	Polyethylene glycol 4,000	50.00	15.00	%w/v	
Buffer	Sodium cacodylate	1.00	0.10	M	6.00

Table 4: Conditions of a possible hit 2 of crystallization trial

Type	**Name**	**Stock Conc.**	**Conc.**	**Units**	**pH**
Precipitant	Polyethylene glycol 4,000	50.00	15.00	%w/v	
Buffer	MES	1.00	0.10	M	6.00
Salt	Ammonium sulfate	4.00	0.15	M	

Both of these hits were carried forward to crystallization optimization experiments. For hit 1 the PEG 4000 concentration was varied from 10% to 25% and the pH of the sodium

cacodylate buffer was varied from pH 5.5 to 6.5. Hit 2 was optimized in an identical fashion except for MES replacing sodium cacodylate. No improvement was observed in these optimization experiments.

3.2.2. Methylation of lysine residues in protein

A possible explanation for the tendency for protein to fail to crystallize might be the presence of surface lysines. The side chains are likely, through entropic effects, to destabilize the crystal lattice (50). The molecular flexibility is detrimental to the formation of a highly ordered crystals lattice. Even the small motions such as those due to flexible, solvent-exposed amino acid side chains can be equally detrimental (50). However, chemical modification of surface lysines reduced the surface entropy, the hydrophobic nature of the dimethylated lysine favored protein-protein interactions (50). There are 3 lysines present in the N-terminal domain. In order to reduce the solubility of the protein and to improve the chances of the crystallization, I carried out the reductive methylation of exposed lysines using dimethlyamne-borane and formaldehyde. After methylation the protein was concentrated to 73 mg/ml and the crystallization trials were set up immediately. Approximately 3 days later I noticed a bar shaped crystal (figure 3.9). The condition of the hit is stated in table 5.

Table 5: Conditions of a chemically modified N-terminal domain that produced a rod shaped crystal

Type	**Name**	**Stock Conc.**	**Conc.**	**Units**	**pH**
Precipitant	Polyethylene	50.00	25.00	%w/v	

	glycol 3,350				
Buffer	BIS-TRIS	1.00	0.10	M	5.50
Salt	Magnesium Chloride	2.50	0.20	M	

3.2.3. Using circular dichroism to evaluate the secondary structure

In order to gain some structural knowledge of N-terminal domain circular dichroism (CD) spectrometry was used to estimate the secondary structure. CD is an exceptional tool for determination of the secondary structure and the folding properties of proteins. It measures differences in the absorption of left-handed polarized light versus right-handed polarized light. UV spectral region from 200-260 nm was used because at these wavelengths the chromophore is the peptide bond, and the signal arises when it is located in a regular, folded environment (51). Alpha helix, beta sheet, and random coil structures each give rise to a characteristic shape and magnitude of CD spectrum (figure 10). The approximate fraction of each secondary structure type that is present in any protein can be determined by analyzing its CD spectrum as a sum of fractional multiples for each structural type (51). The protein's buffer was exchanged with 10 mM sodium phosphate buffer (pH 8.0) because Tris-HCl absorbs strongly in the UV range. The protein used for CD spectrometry had a concentration of 0.2 mg/ml (figure 3.11). Two peaks were noticed at 208 nm and 222 nm, which when compared with the standard spectrum looks largely alpha helical (figure 3.11) in structure (51). The sequence of the N-terminal domain was also analyzed in order to confirm the experimental results, which further confirm that N-terminal is mainly alpha helical (figure 3.12). All the data points of the CD spectrums were taken on the same day. However, the spectrum of a native N-terminal domain and the spectrum of a native N-

terminal domain incubated with urea were taken on different days. The background of each spectrum varies every time. This affected the ellipticity values of the results.

3.2.4. Effects of urea on the stability of N-terminal domain

The stability of N-terminal domain was examined by analysis of samples exposed to increasing concentration of urea. As the urea concentration increased the two peaks that signifies the alpha helical structure start disappearing suggesting that the protein is unfolding. A noticeable loss of secondary structure was observed at 2 M urea concentration and for complete unfolding a concentration of 8 M urea (figure 3.13) was required. A plot of urea concentration vs. the ellipticity at 208 nm revealed a rapid unfolding transition between 4 and 5 M urea, indicating the domain is stably folded (figure 3.14). The decreased ellipticity at lower concentration of urea may be due to the transformation of native form to some intermediate state. This can be due to micro environmental changes in the aromatic region of the protein, small local rearrangements of the native state (52) or the stabilizing effects of urea at low concentration (53,54). There are several reports of urea providing different estimates for the conformational stability of a protein (55,56,57,58,59,60,61).

Figures

Figure 3.1

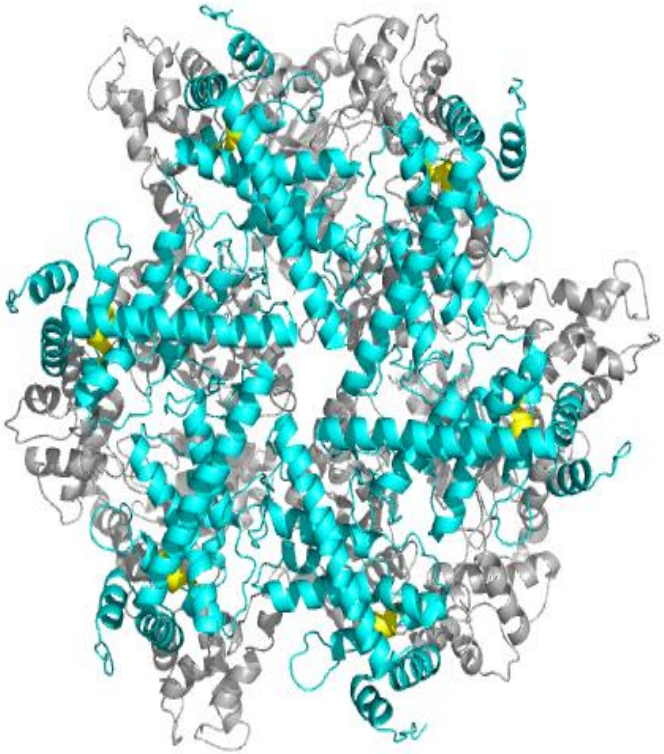

***Figure 3.1*: *Hexameric structure of bacterial FtsH*.** Protease domain is highlighted in cyan color and zinc-binding motifs is highlighted in yellow color

Figure 3.2

Figure 3.2*: *Sequence alignment of i-AAA MyceliophthoraTthermophile with FtsH thermus thermophiles. The amino acids in blue are the negative amino acids; the amino acids in green are the amino acids with polar uncharged side chains. Amino acids in red are with hydrophobic side chains and amino acids in pink are with charged side chains.

Figure 3.3

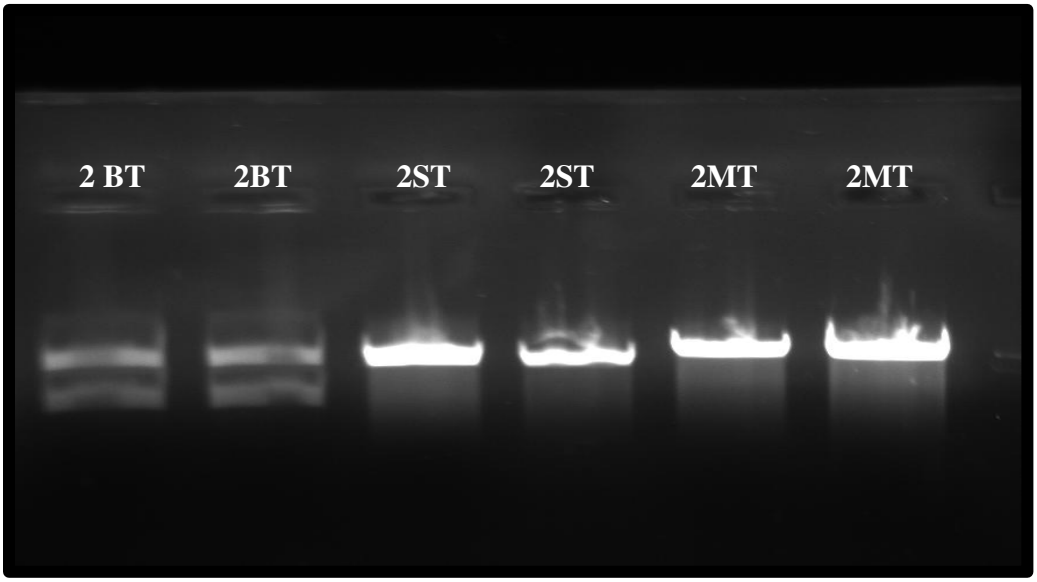

Figure 3.3**:** *Ssp1 treatments of 2BT, 2ST and 2MT Vector*. The treatment linearized the vectors; therefore, a single band is seen on the gel. However, two bands were noticed for 2BT vector probably the enzyme did not cut the 2BT vector efficiently.

Figure 3.4

A.

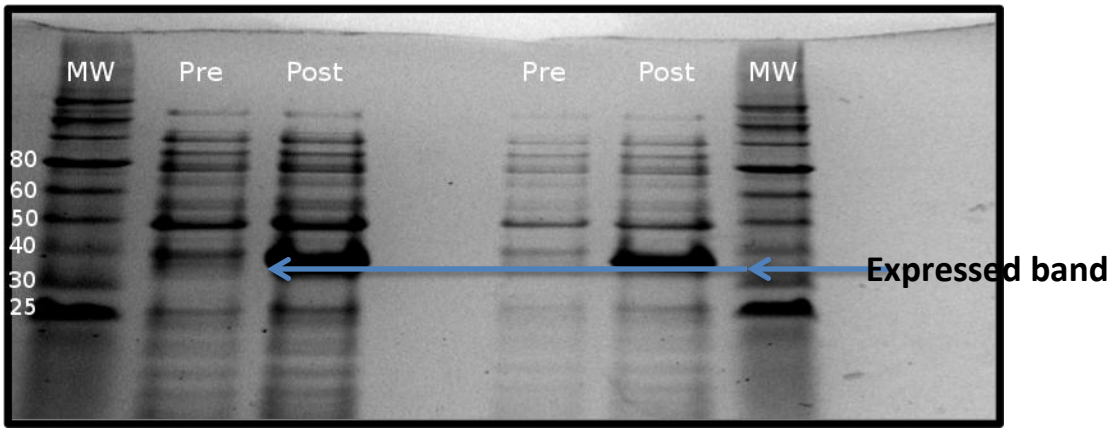

B.

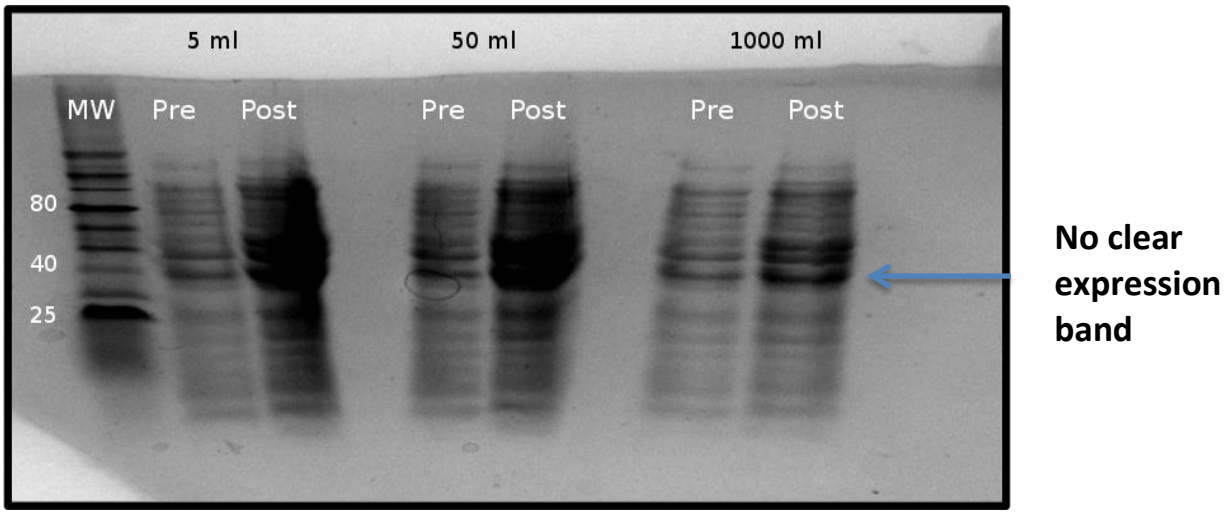

Figure 3.4: *Small-scale expression and large-scale expression of protease domain*. (**A**) A clear band is seen around 38 kDa in the post-induction lane on the Bis-Tris gel (12%) confirming the expression of protease domain at small scale. (**B**) No distinctive band is seen on the SDS-PAGE (12%) in the post-induction lane on the large-scale level that is in 1000 ml lane suggesting an unsuccessful expression

Figure 3.5

A.

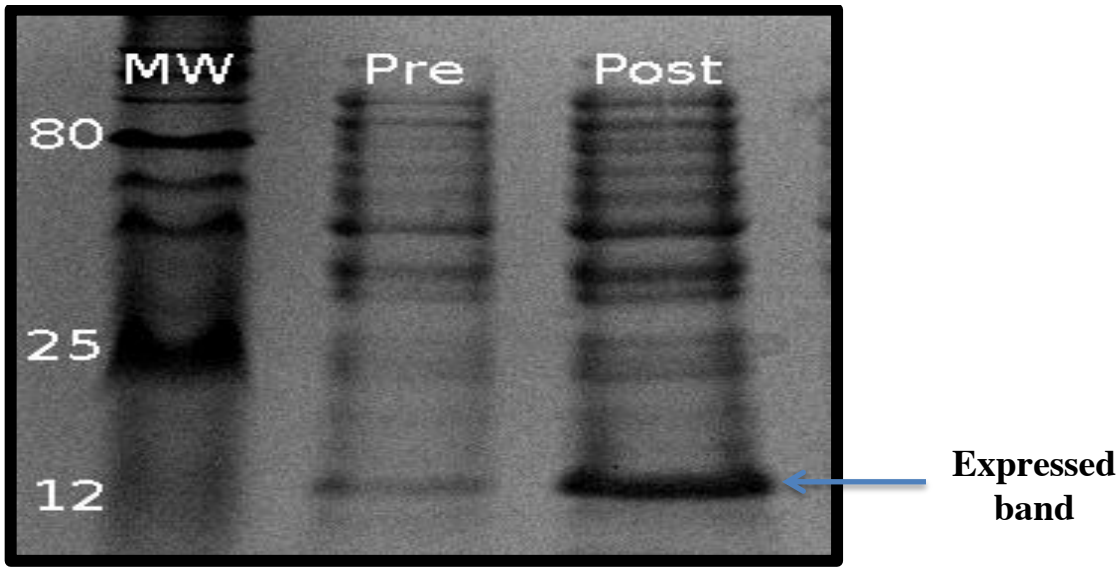

B.

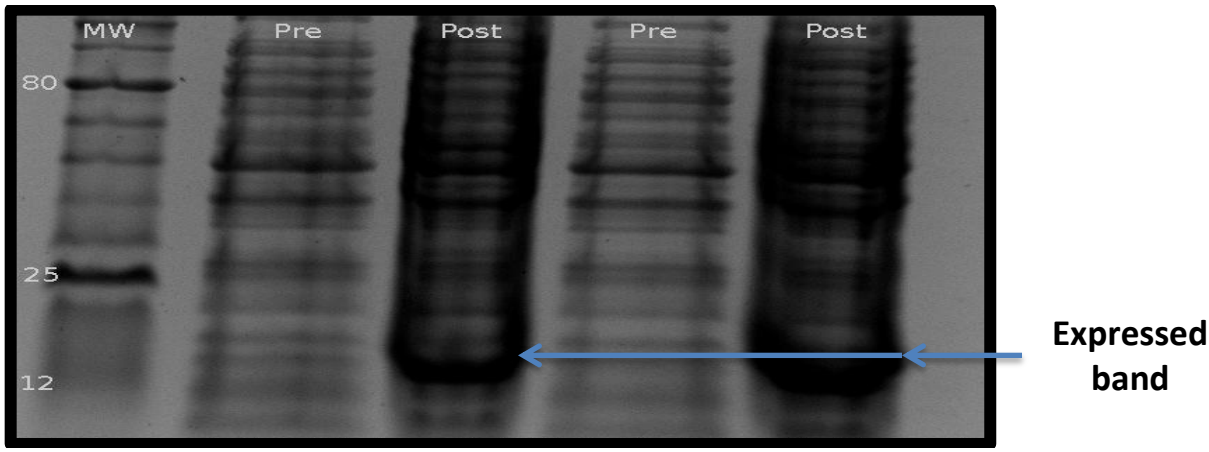

Figure 3.5: *Small-scale expression and large-scale expression of N-terminal domain.* (**A)** A clear band is seen after the induction of the sample with IPTG on a Bis-Tris gel (12%) around 12.42 kDa. This confirms the expression of N-terminal at small-scale level. (**B)** Two liters is expressed at large-scale level and a 10 µl aliquot is taken out before and after the addition of IPTG as pre and post-induction. The samples were resolved on SDS-PAGE (12%). Two thick bands were seen in post-induction lane justify the successful expression at large-scale level.

Figure 3.6

A.

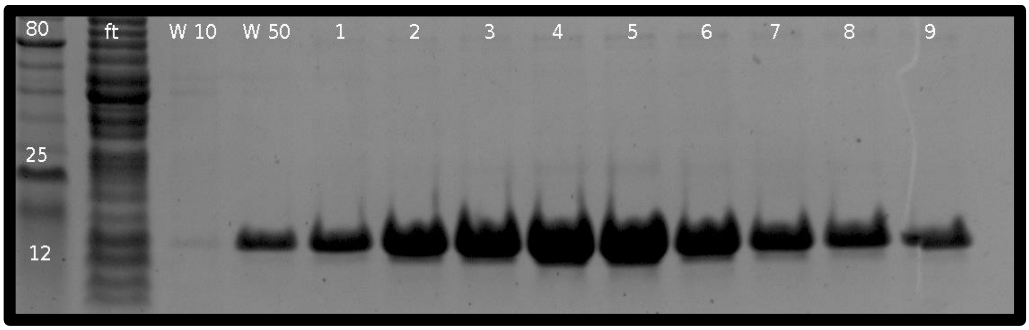

B.

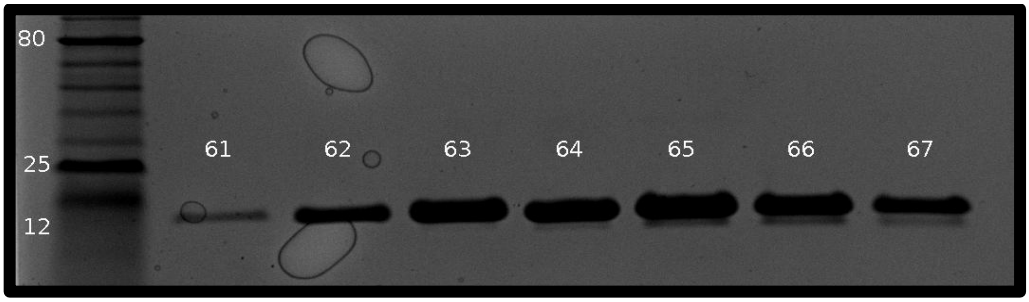

Figure 3.6: *Analysis of N-terminal domain of i-AAA after nickel affinity chromatography and gel filtration*. **(A)**. The sample poured through the column collected and labeled as flow through. Then the column is washed with a buffer containing 10 mM and 50 mM imidazole. The washed sample is also collected. Then the elution buffer is poured and eluted sample is collected in fractions. The collected samples were resolved on SDS-PAGE (12%). The bands were seen at 12.42 kDa. **(B)** Fractions containing the highest concentration of protein collected from the nickel affinity chromatography were mixed together and passed through the superdex 200 column. Fractions corresponding to the peak were collected and 10 µl aliquot from each fraction is resolved on SDS-PAGE (12%).

Figure 3.7

A.

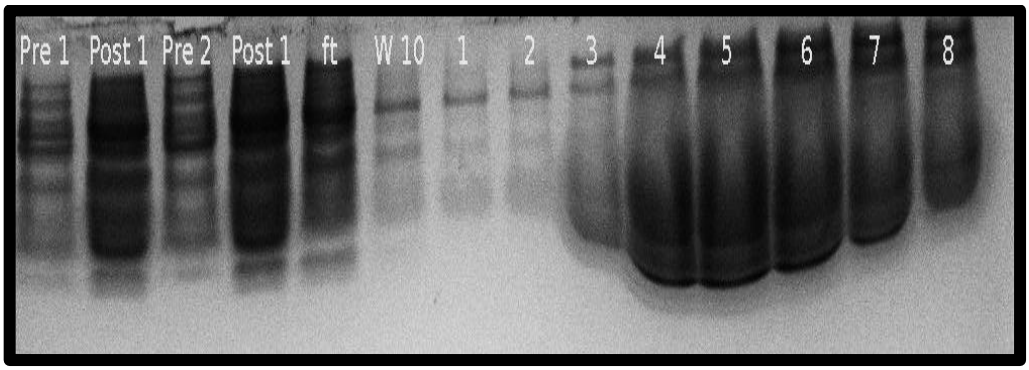

B.

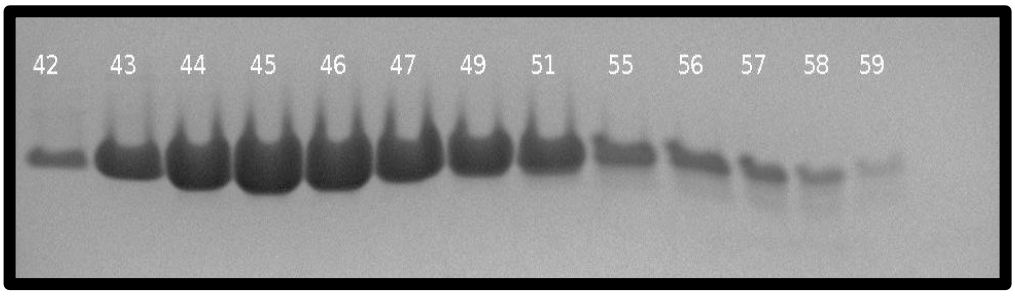

Figure 3.7*: *Analysis of 2 L of N-terminal domain after nickel affinity chromatography and gel filtration. (**A)** A clear dark band is seen in the post-induction column as compared to pre-induction column. The sample is poured in the nickel column and collected and labeled as flow through. The column is washed with a buffer containing 10 mM imidazole. Again the flow through is collected and labeled as washed. Then the elution buffer is poured and eluted sample is collected in fractions. The collected samples were resolved on SDS-PAGE (12%). The later fractions have high amount of protein as compared to earlier fractions in which a clear band id seen. **(B)** Fractions contaning the highest concentrations of protein that were collected from nickel affinity chromatography were mixed tothgether and passed through the superdex 200 column. Fractions corresponding to the peak were collected and a 10 µl is taken out and resolved on the SDS-PAGE (12%). The dark thick bands indicate the presence of large amount of protein.

Figure 3.8

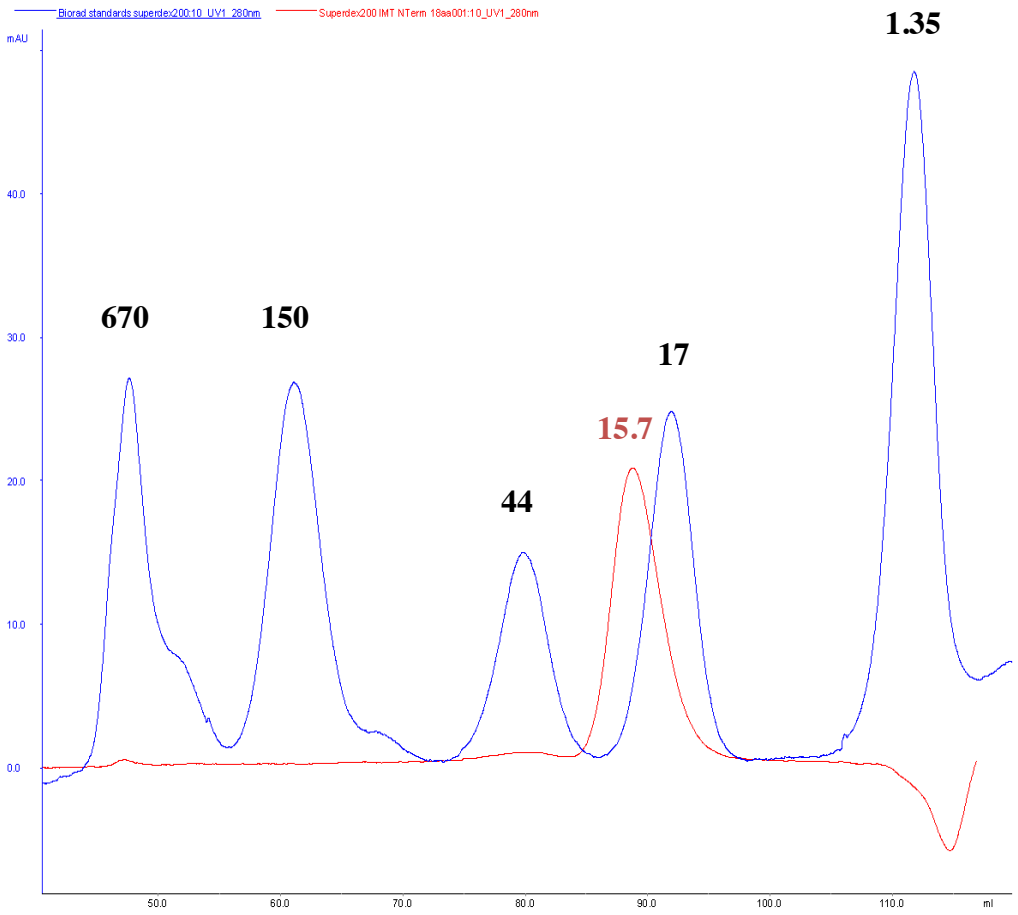

Figure 3.8*: *Gel filtration spectrum of N-terminal domain (red) compared with the standard spectrum of superdex 200 (blue). The molecular weights of the blue peaks are as follow 670 kDa, 150 kDa, 44 kDa, 17 kDa and 1.35 kDa. The molecular weight of the red peak is 15.7 kDa. The N-terminal domain peak is running bigger than its molecular weight on a gel filtration chromatogram

Figure 3.9

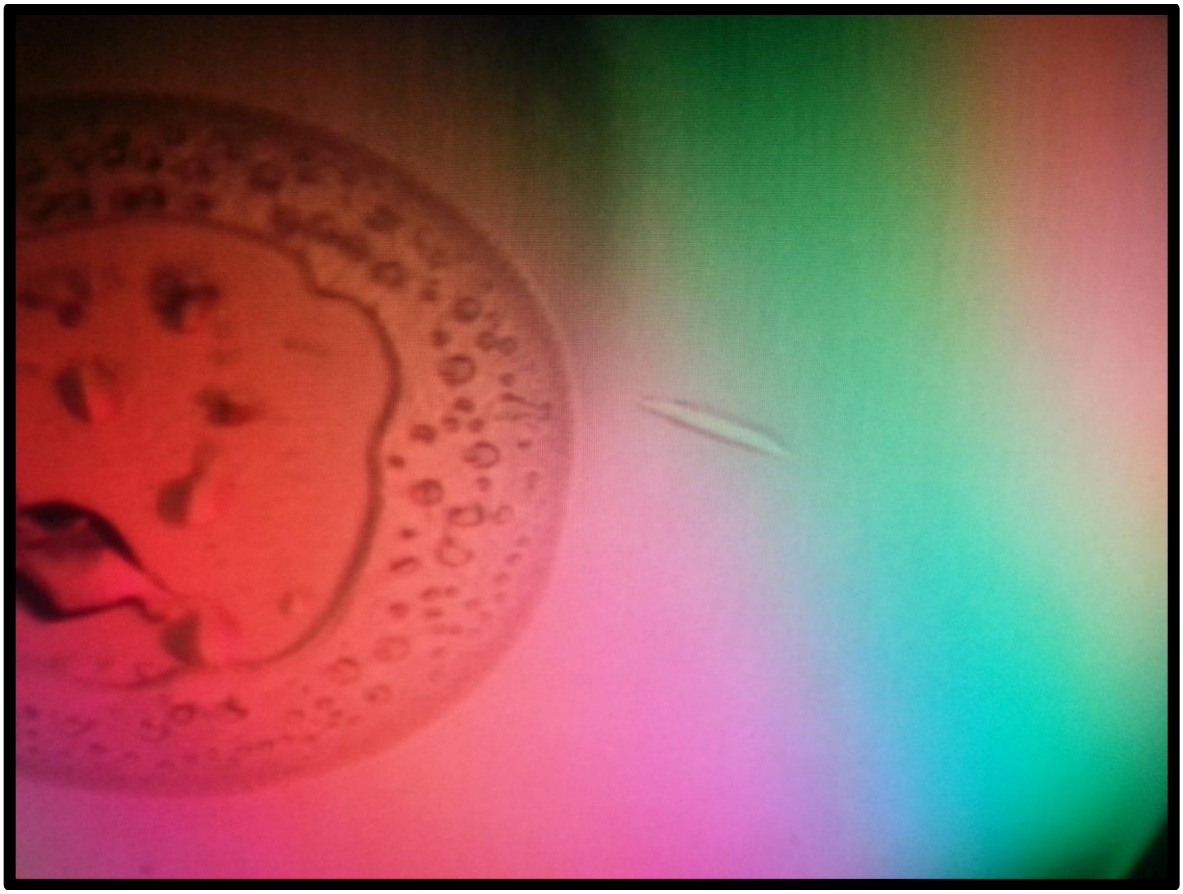

Figure 3.9**:** *A rod-shaped crystal of N-terminal domain*. 3 days after the lysine methylation a bar shaped crystal appears. The condition includes magnesium chloride (0.20 M), Bis-Tris (pH 7) and polyethylene 3,350 (25 %w/v)

Figure 3.10

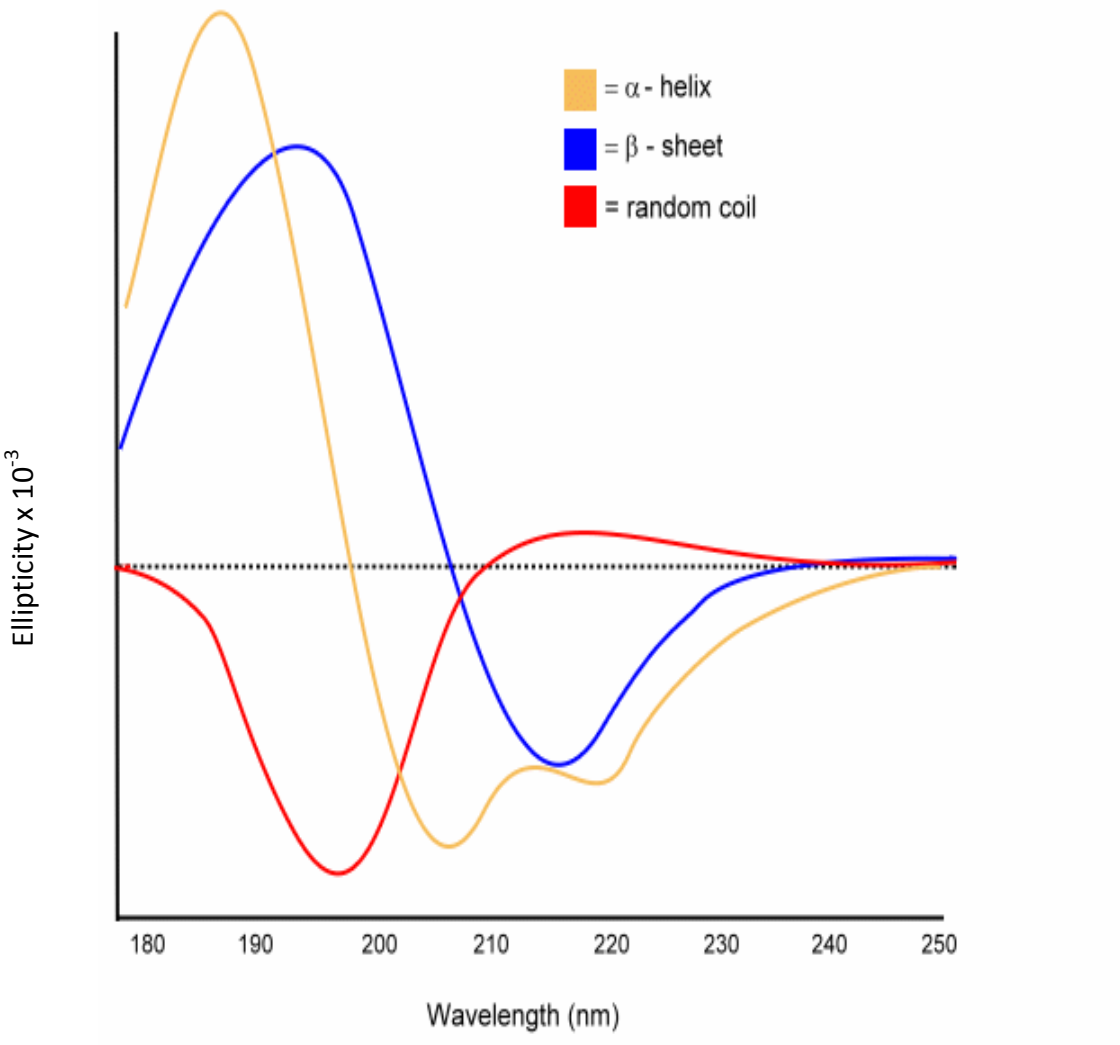

Figure 3.10**:** *Reference spectra of alpha helix, beta-sheet and random coil*. The red spectrum indicates the presence of random coil as the secondary structure. The yellow spectrum indicates the presence of alpha helix as the secondary structure. The blue spectrum indicates the presence of beta-sheet as the secondary structure. The absorption spectrum differs due to long-range order in the amide chromophore.
[Figure adapted from http://www.proteinchemist.com/cd/cdspec.html]

Figure 3.11

A.

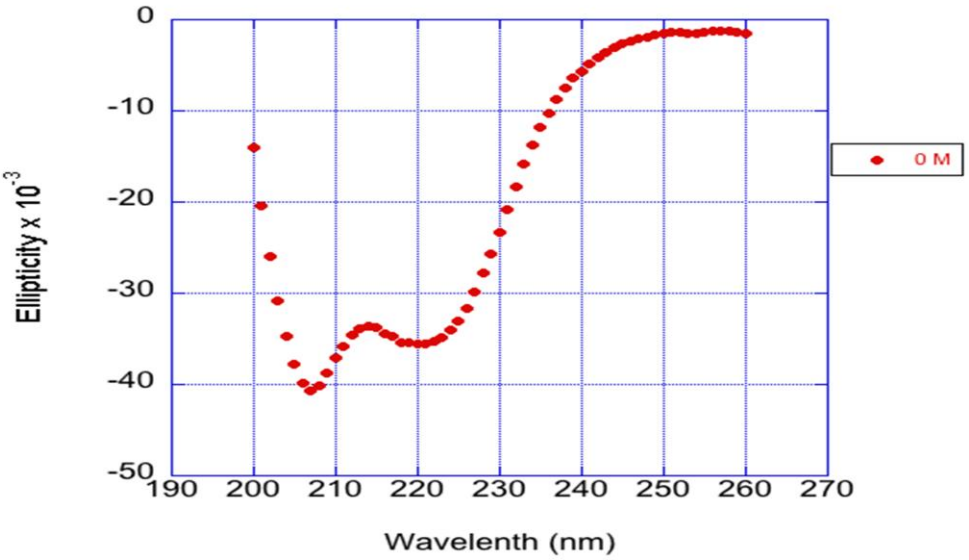

B.

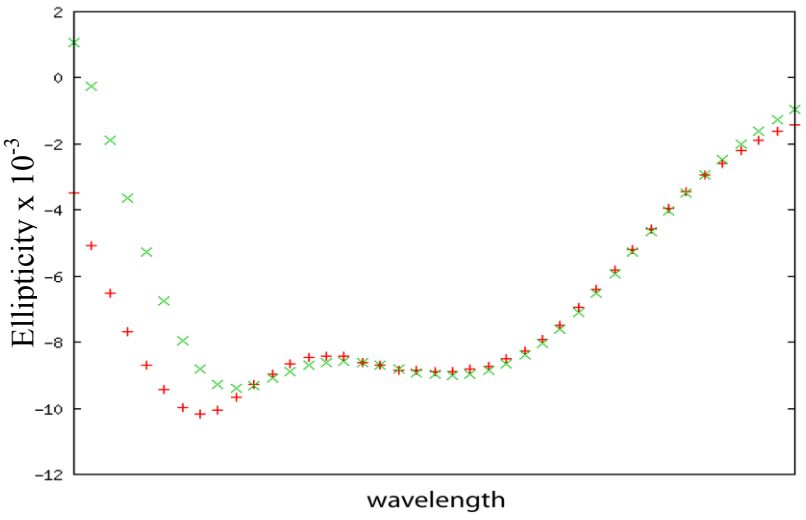

Red = experimental data
Green = standard data

Figure 3.11*: *CD spectrum of N-terminal domain. (**A**) The CD spectrum of native N-terminal shows presence of alpha-helical content. The protein concentration is 0.2 mg/ml. (**B**) CD spectrum of N-terminal domain (red) compared with the standard spectrum of alpha helix (green). The overlapping of the two graphs confirms that the N-terminal is largely alpha-helical. The x-axis is from 200 nm to 260 nm.

Figure 3.12

Figure 3.12**:** *Prediction of the secondary structure of the N-terminal domain of i-AAA*
The N-terminal sequence is highlighted in black and the sequences in red indicate the presence of alpha helices in the N-terminal domain. The sequences in yellow indicate the presence of beta-sheets. From this prediction it can be seen that the N-terminal domain is largely alpha-helical in structure.

Figure 3.13

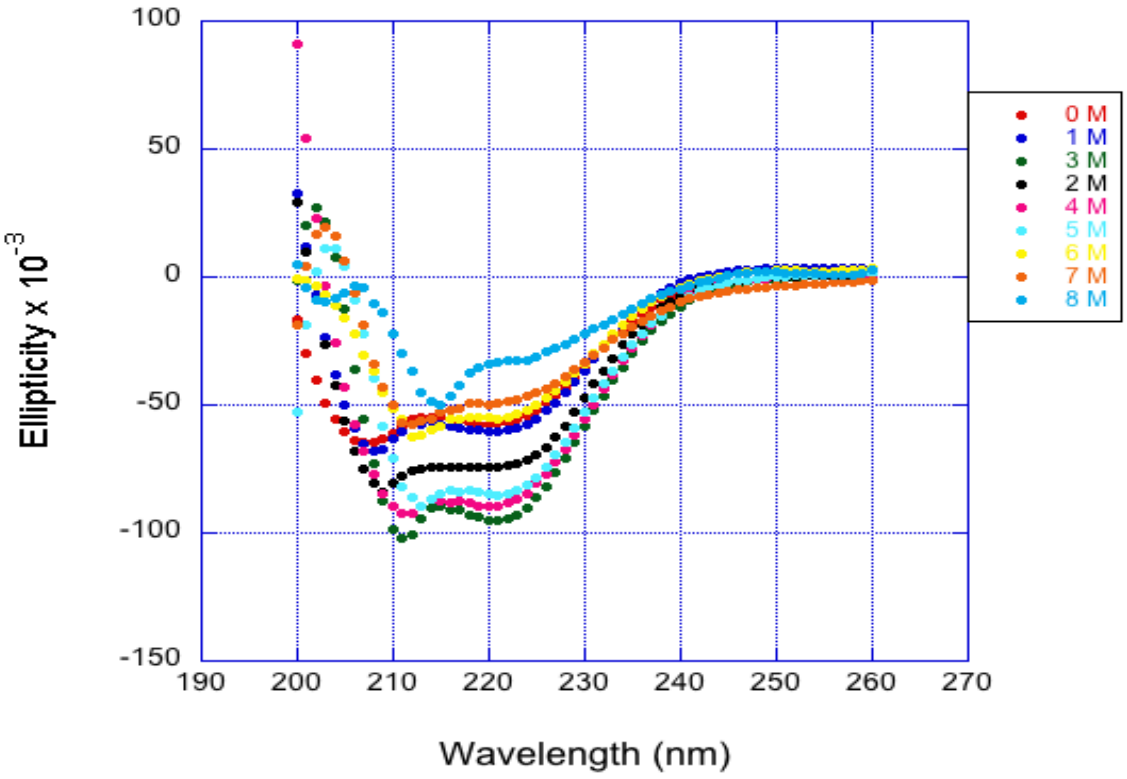

***Figure 3.13*: *Secondary structure analysis of N-terminal domain in the presence of urea*.** Purple spectra indicates the 0 M urea concentration, whereas brown indicates the 8M urea concentration. Native N-terminal domain was incubated with increasing concentration of urea (0-8 M) overnight at room temperature. According to the graph with the increase in the urea concentration the secondary structure of N-terminal domain starts unfolding. Two prominent peaks at 222 nm and at 208 nm start disappearing and the spectrum looks more like a random coil spectrum with a single peak around 215 nm.

Table 6: Data of N-terminal denaturation in urea determined in terms of ellipticity values at wavelength of 208 nm

Urea Concentration (M)	Ellipticity at 208 nm
0	**-64.66**
1	**-67.98**
2	**-80.84**
3	**-73.22**
4	**-77.22**
5	**-39.85**
6	**-36.57**
8	**-33.87**

Figure 3.14

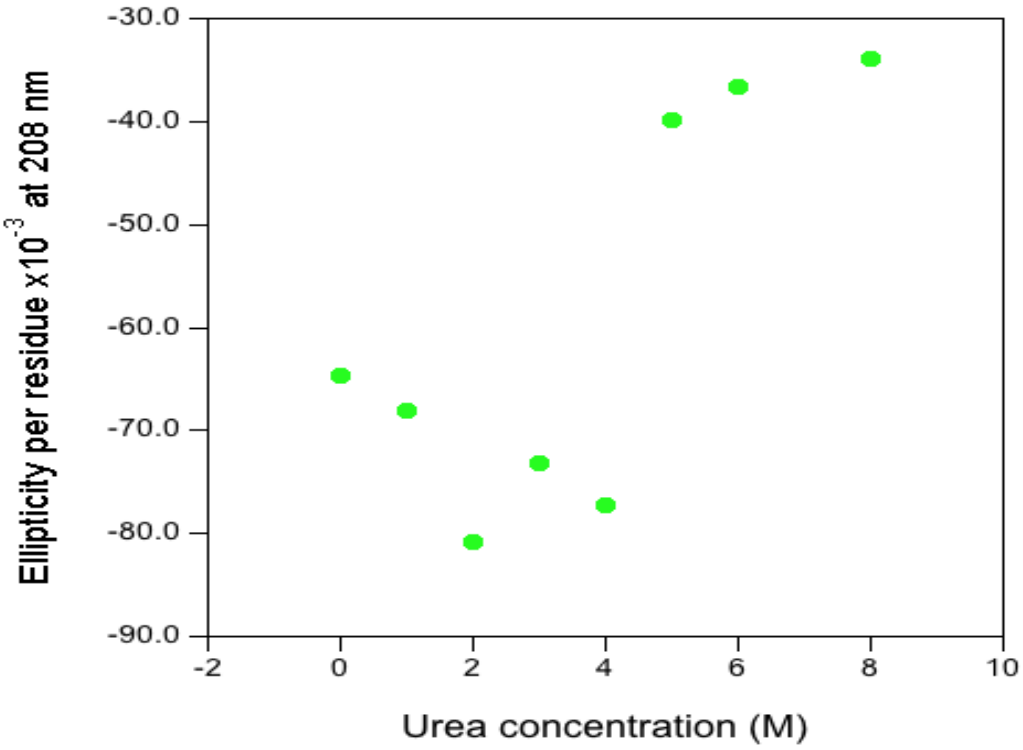

***Figure 3.14*: *Transition curve of N-terminal denaturation in urea determined in terms of ellipticity values at wavelength of 208 nm*.** The ellipticity decreased up to 4 M urea, but increased from 5 M urea.

4. Future Directions

The work presented here has shown that the N-terminal domain of the i-AAA protease from *M*. *Thermophile* adopts a stable alpha-helical structure. Furthermore, methylation of the surface lysine residues has been shown to improve the likely hood of crystallizing this protein. A future direction of this project is to follow up the promising crystallization hit in a series of optimization experiments. These optimizations may yield diffraction quality crystals and enable a full structure determination with this domain. Alternatively, the small size and solubility of the protein makes it an ideal candidate for analysis by nuclear magnetic resonance. Knowledge of the three directional structure may well provide insides into the functional role of the N-terminal domain in the full length i-AAA proteases.

5. References

1. Taylor, R. W., & Turnbull, D. M. (2005) Mitochondrial DNA mutations in human disease. *Nature Reviews Genetics* 6, 389–402
2. Trifunovic, A. et al. (2004) Premature ageing in mice expressing defective mitochondrial DNA polymerase. *Nature* 429, 417–423
3. Muller-Hocker, J. (1990) Cytochrome c oxidase deficient fibres in the limb muscle and diaphragm of man without muscular disease: an age-related alteration. *J. Neurol. Sci.* 100,14–21
4. Mootha, V. K. et al. (2003) PGC-1**α**-responsive genes involved in oxidative phosphorylation are coordinately downregulated in human diabetes. *Nature Genet*. 34, 267–273
5. Petersen, K. F. et al. (2003) Mitochondrial dysfunction in the elderly: possible role in insulin resistance. *Science* 300, 1140–1142
6. Zeviani, M. & Di Donato, (2004) S. Mitochondrial disorders. *Brain* 127, 2153–2172
7. DiMauro, S. & Schon, E. A. (2003) Mitochondrial respiratory-chain diseases. *N. Engl. J. Med*. 348, 2656–2668
8. Shoubridge, E. A. (2001) Nuclear genetic defects of oxidative phosphorylation. Hum. *Mol. Genet*. 10, 2277–2284
9. Thomas Langer , . N.p., n. d. 11 Nov 2013. <http://www.genetik.uni-koeln.de/groups/Langer/proteolysis.html>.
10. Alberts, B. , D. Bray, K. Hopkin, A. Johnson, J. Lewis, M. Raff, K. Roberts, and P. Walter. *Essential cell biology*. 3. Garland Science, 2007. print.
11. "Biological Oxidations and Electron Transport ." *Mitochondrial Membrane Composition*. Oregon University . Web. 13 Nov 2013. http://oregonstate.edu/dept/biochem/hhmi/hhmiclasses/biochem/lectnoteskga/2kfeb04lecturenotes.html
12. Michael Kaser, Thomas Langer. (2000) Protein degradation in mitochondria. *Cell & Developmental Biology* 11: 181-190
13. Leonhard K, Herrmann J M, Stuart R A, Mannhaupt G, Neupert W, Langer T. (1996) AAA proteases with catalytic sites on opposite membrane surfaces comprise a proteolytic system for the ATP-dependent degradation of inner membrane proteins in mitochondria. *EMBO J*. 15:4218–4229
14. Thorsness P E, White K H, Fox T D. Inactivation of *YME1*, a member of the *ftsH-SEC18-PAS1-CDC48* family of putative ATPase-encoding genes, causes increased escape of DNA from mitochondria in *Saccharomyces cerevisiae*. *Mol Cell Biol*. 1993;13:5418–5426
15. Langer T, Neupert W. (1996) Regulated protein degradation in mitochondria. *Experientia* 52: 1069-76
16. Langer T, Leonhard K, Arlt H, Perryman R, Neupert W. (1997) Degradation of membrane proteins by AAA proteases in mitochondria. In: Hopsu-Havu V K, Järvinen M, Kirschke H, editors. Proteolysis in cell functions. Amsterdam, The Netherlands: *IOS Press*; pp. 323–331.
17. Rep M, Grivell L A. (1996) The role of protein degradation in mitochondrial function and biogenesis. *Curr Genet*. 30:367–380.
18. Tzagoloff A, Yue J, Jang J, Paul M F. A new member of a family of ATPase is essential

for assembly of mitochondrial respiratory chain and ATP synthetase complexes in *Saccharomyces cerevisiae*. *J Biol Chem*. 1994;269:26144–26151
19. Suzuki C K, Rep M, Van Dijl J M, Suda K, Grivell L A, Schatz G. (1997) ATP-dependent proteases that also chaperone protein biogenesis. *Trends Biochem Sci*. 22:118–123
20. Guélin E, Rep M, Grivell L A. (1994) Sequence of the *AFG3* gene encoding a new member of the FtsH/Yme1/Tma subfamily of the AAA-protein family. *Yeast* 10:1389–1394
21. Pajic A, Tauer R, Feldmann H, Neupert W, Langer T. (1994) Yta10p is required for the ATP-dependent degradation of polypeptides in the inner membrane of mitochondria. *FEBS Lett*. 353:201–206.
22. Ryoji Suno, Hajime Niwa, Daisuke Tsuchiya, Xiaodong Zhang, Masasuke Yoshida, Kosuke Morikawa (2006) Structure of the Whole Cytosolic Region of ATP-Dependent Protease FtsH. *Molecular Cell* 22: 575-585
23. Arlt H, Tauer R, Feldmann H, Neupert W, Langer T. (1996) The YTA10-12-complex, an AAA protease with chaperone-like activity in the inner membrane of mitochondria. *Cell* 85:875–885
24. Michael J. Baker, Ved P. Mooga, Bernard Guiard, Thomas Langer, Michael T. Ryan, Diana Stojanovski (2012) Impaired Folding of the Mitochondrial Small TIM Chaperones Induces Clearance by the *i*-AAA Protease. *Molecular Biology* 424(5): 227–239
25. Leonhard K et al (1999) Chaperone-like activity of the AAA domain of the yeast Ymel AAA protease. *Nature* 398:348–351
26. Stinson BM, Nager AR, Glynn SE, Schmitz KR, Baker TA, Sauer RT (2013) Nucleotide binding and conformational switching in the hexameric ring of a AAA+ machine. *Cell* 153(3): 628-39
27. John Carroll, Ilona Miko. N.p.. Web. 11 Nov 2013. <http://www.nature.com/scitable/topicpage/mitochondria-14053590>.
28. Martin Graef, Georgeta Seewald, Thomas Langer. (2007) Substrate Recognition by AAA + ATPases: Distinct Substrate Binding Modes in ATP-Dependent protease Yme 1 of the Mitocnondrial Intermembrane Space. *Mol*. *Cell*. *Biol*. 27(7): 2476
29. Tauer R et al (1994) Yta10p, a member of a novel ATPase family in yeast, is essential for mitochondrial function. *FEBS Lett* 353:197–200
30. Schnall R et al (1994) Identi**fi**cation of a set of yeast genes coding for a novel family of putative ATPases with high similarity to consitutents of the 26S protease complex. *Yeast* 10:1141–1155
31. Arlt H et al (1998) The formation of respiratory chain complexes in mitochondria is under the proteolytic control of the **m**-AAA protease. *EMBO J* 17:4837–4847
32. Van Dyck L, Langer T (1999) ATP-dependent proteases controlling mitochondrial function in the yeast Saccharomyces cerevisiae. *Cell Mol Life Sci* 56(9-10): 825-42
33. Michael Kaser, Thomas Langer. (2000) Protein degradation in mitochondria. *Cell & Developmental Biology* 11: 181-190
34. Paul MF, Tzagoloff A (1995) Mutations in RCA1 and AFG3 inhibits F**1**-ATPase assembly in Saccharomyces cerevisiae. *FEBS Lett* 373:66–70
35. Casari G et al (1998) Spastic paraplegia and OXPHOS impairment caused by mutations in paraplegin, a nuclearencoded mitochondrial metalloprotease. *Cell* 93:973–983
36. Ban**fi** S et al (1999) Identi**fi**cation and characterization of AFG3L2, a novel paraplegin-

related gene. *Genomics* 59:51–58
37. Wang K, Jin M, Liu X, Klionsky DJ. (2013) Proteolytic processing of Atg32 by the mitochondrial i-AAA protease Yme1 regulates mitophagy. *Autophagy* 9:11
38. Weber ER, Hanekamp T, Thorsness PE (1996) Biochemical and functional analysis of the YME1 gene product, an ATP and zinc-dependent mitochondrial protease from S. cerevisiae. *Mol Biol* Cell 7:307–317
39. Pearce DA, Sherman F (1995) Degradation of cytochrome oxidase subunits in mutants of yeast lacking cytochrome c and suppression of the degradation by mutation of yme1. *J Biol Chem* 270:1–4
40. Nakai T et al (1995) Multiple genes, including a member of the AAA family, are essential for the degradation of unassembled subunit 2 of cytochrome c oxidase in yeast mitochondria. *Mol Cell Bio* 15:4441–4452
41. Carla Koehler, Matthias F. Bauer. (2004) Mitochondrial Function and Biogenesis. *Springer* 8:103-104
42. Atorino L et al (2003) Loss of m-AAA protease in mitochondria causes complex I deficiency and increased sensitivity to oxidative stress in hereditary spastic paraplegia. *J Cell Bio* 163(4):777-87
43. Hinnerwisch, J., B. G. Reid, W. A. Fenton, and A. L. Horwich. (2005). Roles of the N-domains of the ClpA unfoldase in binding substrate proteins and in stable complex formation with the ClpP protease. *J. Biol. Chem.* 280:40838-40844
44. Thorsness PE, White KH, Fox TD (1993) Inactivation of YME1, a member of the ftsH-SEC18-PAS1-CDC48 family of putative ATPase-encoding genes, causes increased escape of DNA from mitochondria in Saccharomyces cerevisiae. *Mol Cell Bio* 13:5418–5426
45. Campbell CL et al (1994) Mitochondrial morphological and functional defects in yeast caused by yme1 are suppressed by mutation of a 26S protease subunit homologue. *Mol Biol Cell* 5:899–905
46. Rayment I. (1997) Reductive alkylation of lysine residues to alter crystallization properties of proteins. *Methods Enzymol* 276:171-179
47. Thomas S. Walter et al. (2006) Lysine Methylation as a routine rescue strategy for protein crystallization. *Structure* 14: 1617-1622
48. Altschul, S.F., Gish, W., Miller, W., Myers, E.W. & Lipman, D.J. (1990) "Basic local alignment search tool." J. Mol. Biol. 215:403-410.
49. Goujon M, McWilliam H, Li W, Valentin F, Squizzato S, Paern J, Lopez R. (2010) A new bioinformatics analysis tools framework at EMBL-EBI. *Nucleic acids research 2010 Jul, 38 Suppl: W695-9*
50. Norma J Greenfield (2007) Using circular dichroism spectra to estimate protein secondary structure. *Nature* 2876-2890
51. Perez-Iratxeta C, Andrade-Navarro MA. (2007). K2D2: estimate of protein secondary structure from circular dichroism spectra. *BMC Struct Biol*, 8-25
52. Ferreon, A. C., and Bolen, D. W. (2004). Thermodynamics of denaturant-induced unfolding of a protein that exhibits variable two-state denaturation. *Biochemistry* 43:(42) 3357–13369
53. Mayr, L. M., and Schmid, F. X. (1993). Stabilization of a protein by guanidinium chloride. *Biochemistry* 32:7994–7998
54. Smith, J. S., and Scholtz, J. M. (1996). Guanidine hydrochloride unfolding of peptide

helices: separation of denaturant and salt effects. *Biochemistry* 35: 7292–7297
55. Pace, C. N. (1986) Determination and analysis of urea and guanidine hydrochloride denaturation curves. *Methods Enzymol*. 131: 266–280
56. Yao, M., and Bolen, D. W. (1995). How valid are denaturant-induced unfolding free energy measurements? Level of conformance to common assumptions over an extended ranges of ribonuclease A stability. *Biochemistry* 34: 3771–3781
57. Inouye, K., Tanaka, H., and Oneda, H. (2000). States of tryptophyl residues and stability of recombinant human matrix metalloproteinase 7 (matrilysin) as examined by fluorescence *J*. *Biochem*.*(Tokyo)* 128:(3), 363–369
58. Wang, G. F., Cao, Z. F., Zhou, H. M., and Zhao, Y. F. (2000). Comparison of inactivation and unfolding of methanol dehydrogenase during denaturation in guanidine hydrochloride and urea. *Int*.*J*. *Biochem*. *Cell Biol*. 32: 873–878.
59. Deshpande, R. A., Khan, M. I., and Shankar, V. (2003). Equilibrium unfolding of RNase Rs from Rhizopus stolonifer: pH dependence of chemical and thermal denaturation. *Biochm*.*Biophys*. *Acta* 1648:(1–2), 184–194.
60. Inui, T., Okhubo, T., Emi, M., Irikura, D., Hayaishi, O., and Urade, Y. (2003). Characterization of the unfolding process of lipocalin-type prostaglandin D synthase. *J*. *Biol*.*Chem*. 278:(5), 2845–2852.
61. Park, Y. D., Jung, J. Y., Kim, D. W., Kim, W. S., Hahn, M. J., and Yang, J. M. (2003). Kinetic inactivation study of mushroom tyrosinase: intermediate detection by denaturants. *J*. *Protein Chem*. 22:(5), 463–471.